Catalysis Science & Technology

PAPER

View Article Online
View Journal | View Issue

Cite this: *Catal. Sci. Technol.*, 2014, 4, 1151

BF_3/MCM-41 as nano structured solid acid catalyst for the synthesis of 3-iminoaryl-imidazo[1,2-a]pyridines

Mohammad Abdollahi-Alibeik* and Ali Rezaeipoor-Anari

Received 20th November 2013,
Accepted 19th January 2014

DOI: 10.1039/c3cy00947e

www.rsc.org/catalysis

Multi-component reaction of various types of aldehydes, 2-aminopyridines and trimethylsilyl cyanide was carried out in the presence of MCM-41 supported boron trifluoride (BF_3/MCM-41) as a nanostructured solid acid catalyst for the synthesis of 3-iminoaryl-imidazo[1,2-a]pyridine derivatives. MCM-41 nanoparticles were synthesized by a sol–gel method and BF_3/MCM-41 samples with various loading amounts of BF_3 and different calcination temperatures were prepared and characterized by XRD, SEM and FT-IR techniques. The catalytic performance experiments show that BF_3/MCM-41 calcined at 400 °C has the best catalytic activity. The recyclability and reusability experiments show that the catalyst is reusable many times with a moderate decrease in activity.

1. Introduction

Compounds with an imidazo[1,2-a]pyridine scaffold have been shown to possess a broad spectrum of biological activities, such as anti-inflammatory,[1,2] antifungal,[3] antiviral,[4] anticonvulsant[5] and hypnotic[6] activity. The general method for the synthesis of imidazo[1,2-a]pyridines involves isocyanide-based multi-component condensation reactions of various isocyanides, aldehydes and 2-aminopyridines in the presence of various catalysts and conditions, such as synthesis of 3-aminoimidazo[1,2-a]azines in the presence of supported scandium triflate on solid,[7] combinatorial synthesis of fused 3-aminoimidazoles[8] and Ugi reaction for synthesis of 3-aminoimidazo[1,2-a]pyridines and imidazo[1,2-a]pyrazines.[9] Recently, a new protocol has been developed for the synthesis of imidazo[1,2-a]pyridines using trimethylsilyl cyanide (TMSCN) as a traditional cyanide source instead of isocyanide.[10,11] This new protocol is analogous to the classical Strecker and Ugi reactions; however, microwave irradiation is required.

Since the discovery of the latter method, many catalytic systems have been developed for the multi-component reaction of TMSCN, aldehydes and 2-aminopyridines, such as 1-butyl-3-methylimidazolium bromide [Bmim][Br][12] and silica–sulfuric acid.[13]

The use of solid acid catalysts has attracted considerable attention in organic transformations due to their advantages such as ease of handling, simple work-up and reusability of the catalyst. A possibility for developing solid acids is surface modification of solid supports such as mineral oxides.

Among them, MCM-41 with highly ordered hexagonal mesopores (1–10 nm), high surface area (~1000 $m^2\ g^{-1}$) and high thermal stability has been the focus of recent applications of catalysts and catalyst supports.[14–20]

In this paper we aim to report the preparation, characterization and catalytic application of MCM-41 supported boron trifluoride (BF_3/MCM-41) as a solid acid catalyst for the synthesis of imidazo[1,2-a]pyridines by a one pot, multi-component reaction of TMSCN, aldehydes and 2-aminopyridines (Scheme 1).

2. Experimental

2.1. Material and methods

All chemicals were commercial products. All reactions were monitored by TLC and all yields refer to isolated products. Melting points were obtained on Buchi B-540 apparatus and are uncorrected. ^1H and ^{13}C NMR spectra were recorded in DMSO-d_6 on a Bruker Avance III 400 (400 MHz for ^1H and 100 MHz for ^{13}C) spectrometer. Infrared spectra of the catalysts and reaction products were recorded on a Bruker FT-IR Equinax-55 spectrophotometer in KBr pellets. XRD patterns were recorded on a Bruker D8 ADVANCE X-ray diffractometer using nickel filtered Cu Kα radiation (λ = 1.5406 Å). The morphology was studied using a Philips XL30 scanning electron microscopy. A Metrohm 691 pH meter with a Metrohm fluoride ion-selective electrode (6.0502.120) coupled with Metrohm reference electrode Ag/AgCl (6.0729.100) was used for fluoride determination.

Department of Chemistry, Yazd University, Yazd 89195-741, Iran.
E-mail: abdollahi@yazduni.ac.ir; Fax: +98 351 8210644; Tel: +98 351 8122659

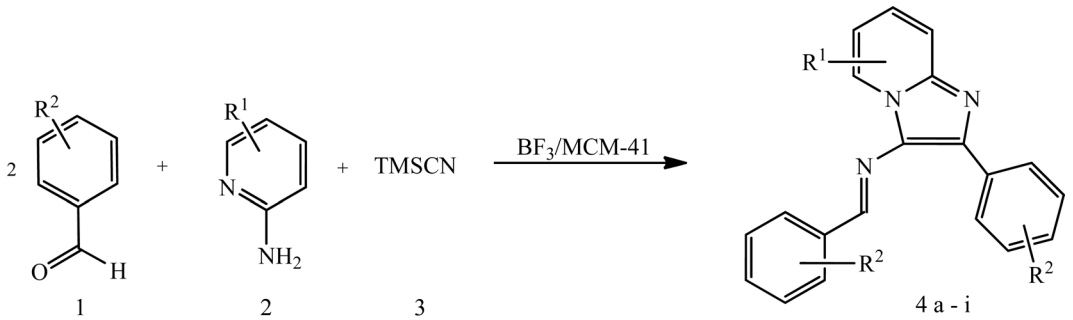

Scheme 1

2.2. Preparation of MCM-41 nanoparticles

The synthesis of nanosized MCM-41 was carried out using tetraethylorthosilicate (TEOS) as the Si source, cetyltrimethylammonium bromide (CTAB) as the template and ammonia as the pH control agent with the gel composition of SiO_2: CTAB : NH_4OH : H_2O = 1 : 0.127 : 1.261 : 476.5.

In a typical procedure, 1.04 g of CTAB was added to deionized water (200 mL) at 70 °C and then 5 mL TEOS was added dropwise for 1 h and the mixture was allowed to cool to room temperature. Then aqueous ammonia (25 wt.%) was added until the pH of the solution was adjusted to 10.5 and the mixture was stirred for 12 h. The gel was separated by centrifuge and washed with distilled water (20 mL) and EtOH (2 × 10 mL), respectively. The gel was dried in an oven at 120 °C for 1 h and then calcined at 550 °C for 4 h.

2.3. Preparation of BF_3/MCM-41

A mixture of MCM-41 (1 g), toluene (10 mL) and $BF_3{\cdot}Et_2O$ (3 mmol) was stirred for 12 h at room temperature. The suspension was separated by centrifuge and washed with toluene (10 mL). The solid was dried in an oven at 120 °C for 1 h and then calcined at 120, 200, 300, 400 or 500 °C for 2 h. The obtained samples were denoted as BM-120, BM-200, BM-300, BM-400 and BM-500, respectively.

2.4. General procedure for the synthesis of imidazo[1,2-a]pyridines in the presence of BF_3/MCM-41

A mixture of 2-aminopyridine (1.1 mmol), aromatic aldehyde (2 mmol), TMSCN (1 mmol) and BM-400 (50 mg) was refluxed in EtOH (2 mL). After completion of the reaction (monitored by TLC, eluent: *n*-hexane : EtOAc, 8 : 2), the catalyst was separated and washed with EtOH (3 × 2 mL). After addition of water, the product was precipitated with high purity. Further purification was achieved by recrystallization in EtOH. The pure imidazo[1,2-a]pyridines were obtained in 75–95% yields.

2.5. Physical and spectroscopic data for selected compounds

4a: m.p.: 160–163 °C, FT-IR (KBr) ν_{max}: 3042, 2927, 1606, 1598, 1499, 1447, 1351, 1241, 1241, 1028, 690 cm^{-1}.

4b: m.p.: 135–138 °C, FT-IR (KBr) ν_{max}: 3050, 2950, 1601, 1520, 1445, 1390, 1233,1021, 690, cm^{-1}; ^1H NMR (400 MHz, $CDCl_3$): δ = 3.02 (s, 3H), 6.57 (d, 1H, J = 4.8 Hz), 7.09 (t, 1H, J = 6.6 Hz), 7.32 (d, 1H, J = 5.4 Hz), 7.40 (t, 2H, J = 5.5 Hz), 7.46 (m, 4H), 7.71 (d, 2H J = 5.2 Hz), 7.75 (d, 2H J = 5.4 Hz), 8.51 (s, 1H).

4c: m.p.: 200–204 °C, IR (KBr) ν_{max}: 3090, 3035, 1606, 1572, 1500, 1487, 1447, 1408, 1399, 1277, 1233, 1193, 1078, 1023, 821, 765, 700 cm^{-1}; ^1H NMR (400 MHz, $CDCl_3$): δ = 6.97 (t, 1H, J = 6.4 Hz), 7.33 (t, 1 H, J = 8.8 Hz), 7.42 (t, 2H, J = 6.0 Hz), 7.64 (d, 1H, J = 8.4 Hz), 8.17 (d, 1H, J = 8.0 Hz), 8.22 (d, 1 H, J = 7.2 Hz), 8.47 (d, 1H, J = 7.2 Hz), 8.65 (m, 1H), 8.71 (m, 1H), 8.8 (s, 1H), 8.96 (s, 1H), 9.1 (s, 1H); ^{13}C NMR (100 MHz, $CDCl_3$): δ = 113.13, 117.71, 123.48, 123.76, 123.84, 126.04, 128.98, 130.86, 131.85, 134.51, 135.81, 143.78, 149.20, 149.43, 150.34, 152.01, 153.43.

4d: m.p.: 155–157 °C, IR (KBr) ν_{max}: 3080, 1600, 1507, 1478, 1247, 1214, 827, 749 cm^{-1}.

4e: m.p.: 172–176 °C, IR (KBr) ν_{max}: 3080, 1600, 1570, 1535, 1512, 1247. 1160. 1021, 783 cm^{-1}.

4f: m.p.: 158–160 °C, IR (KBr) ν_{max}: 3035, 1740, 1363, 1217, 1033, 1214 cm^{-1}; ^1H NMR (400 MHz, $CDCl_3$): δ = 6.90 (t, 1H, J = 4.8 Hz), 7.15 (m, 4H, J = 6.0 Hz), 7.25 (d, 1H, J = 6.9 Hz), 7.81 (m, 4H), 8.42 (d, 1H, J = 5.0 Hz), 8.71 (s, 1H).

4g: m.p.: 135–138 °C, IR (KBr) ν_{max}: 3031, 1641, 1606, 1493, 1271, 730, 690 cm^{-1}; ^1H NMR (400 MHz, $CDCl_3$): δ = 2.44 (s, 3H), 6.72 (d, 1H, J = 4.2 Hz), 7.34 (s, 2H), 7.46 (m, 5H), 7.82 (m, 4H), 8.34 (d, 1H, J = 4.8 Hz), 8.77 (s, 1H).

4h: m.p.: 211–213 °C, IR (KBr) ν_{max}: 3070, 1656, 1604, 1484, 1450, 1240, 1038, 749 cm^{-1}.

4i: m.p.: 150–152 °C, IR (KBr) ν_{max}: 3041, 1640, 1590, 1520, 1491, 1231, 1089, 832 cm^{-1}; ^1H NMR (400 MHz, $CDCl_3$): δ = 2.44 (s, 3H), 6.74 (d, 1H, J = 5.1 Hz), 7.33 (s, 1H), 7.43 (t, 4H, J = 6.3 Hz), 7.77 (d, 4H, J = 5.0 Hz), 8.30 (d, 1H, J = 5.4 Hz), 8.69 (s, 1H).

3. Results and discussions

3.1. Catalyst characterization

Particle morphology of MCM-41 and BM-400 was studied by scanning electron microscopy (SEM). The SEM images show

spherical MCM-41 and BM-400 nanoparticles with a size of <100 nm (Fig. 1).

The FT-IR spectra of MCM-41, BM-120 and BM-400 are shown in Fig. 2. As shown in Fig. 2a, MCM-41 shows characteristic peaks at 1200, 1082 and 810 cm^{-1}, which are assigned to asymmetric and symmetric stretching vibrations of Si–O–Si, and a weaker peak at 966 cm^{-1} due to Si–OH groups.[21,22] The peak at 460 cm^{-1} is assigned to the bending vibration of Si–O–Si. In the spectra of BM-120 and BM-400 (Fig. 2b, c), apart from the main peaks of MCM-41, there are peaks at 1392 and 1408 cm^{-1}, which are assigned to B–O stretching of BM-120 and BM-400, respectively.[23] In the spectrum of BM-400, an increase in the intensity of the peak at 966 cm^{-1} relative to the same peak in the spectrum of BM-120 may be due to an increase in the number of Brønsted sites (Si–OH) provided during B–O covalent bond formation after calcination.

The low angle XRD patterns of MCM-41, BM-120 and BM-400 are shown in Fig. 3. The characteristic peaks of MCM-41 are at 2θ = 2.3°, 4° and 4.6° (Fig. 3a).[21,24] In Fig. 3b and c, after BF_3 loading, the intensity of main peak was decreased and width of the peak was increased in both BM-120 and BM-400 samples. This is due to a decrease in the long-range order of the hexagonal array of mesostructure of MCM-41 after loading of BF_3 into the mesoporous channels of MCM-41. However, an increase in sharpness and intensity of these peaks was observed in the pattern of BM-400, which is a result of the regulation of mesostructure of BM-400 relative to BM-120 (Fig. 2c), maybe due to covalent bonding between boron and SiOH of MCM-41 during calcination.

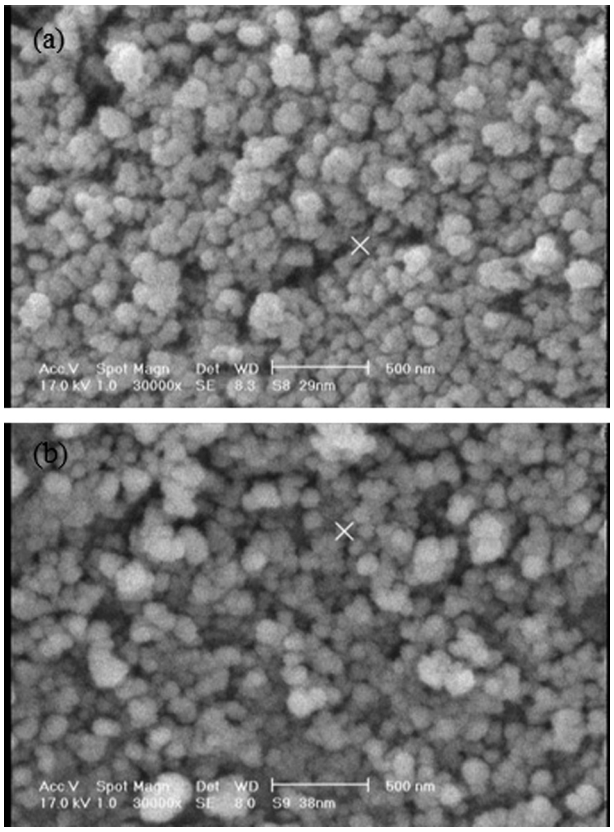

Fig. 1 The SEM image of (a) MCM-41 and (b) BM-400.

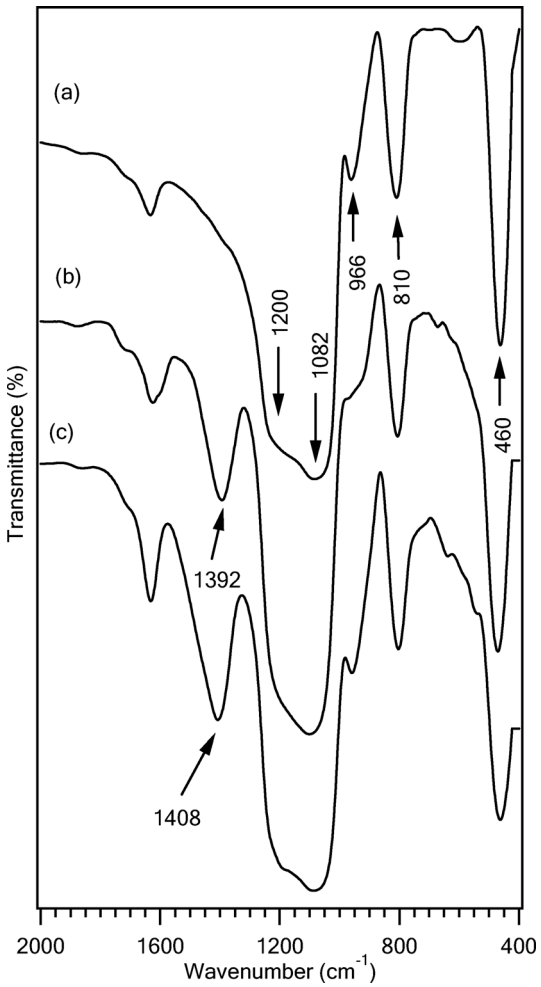

Fig. 2 FT-IR spectra of (a) MCM-41, (b) BM-120 and (c) BM-400.

The catalytic acidity was determined by potentiometric titration of samples with 0.02 N solution of *n*-butyl amine in acetonitrile. According to this method, the initial electrode potential (E_i) indicates the maximum acid strength and the range of where a plateau is reached (meq of the used *n*-butyl amine per gram of the catalyst) indicates the total number of acid sites.[25] As shown in Fig. 4a, the very low initial potential shows that the acid strength of BM samples is higher than MCM-41. As shown in Fig. 4, the strength of BM-200 and BM-300 is close to BM-400 but with a higher number of acid sites than BM-400. These results may be due to leaching of non-bonded BF_3 into solution at lower calcination temperatures. However, a lower initial potential for BM-500 shows weaker acid strength for this sample, which is in agreement with its catalytic activity.

The distribution of both Lewis and Brønsted acid sites of BM-400 was investigated using FT-IR spectroscopy by means of pyridine absorption. The results are shown in Fig. 5. The FT-IR spectrum of pyridine-adsorbed BM-400 before heat treatment

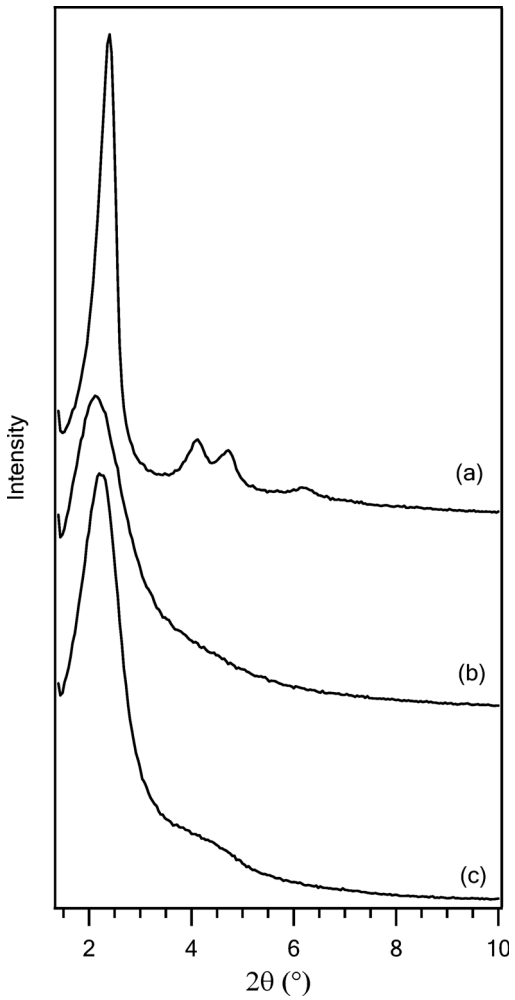

Fig. 3 XRD patterns of (a) MCM-41, (b) BM-120 and (c) BM-400.

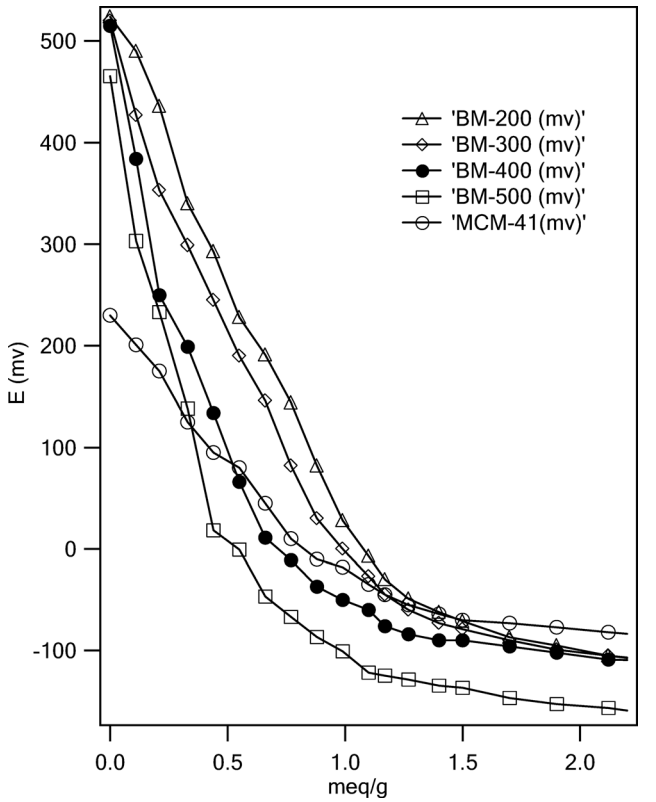

Fig. 4 Potentiometric titration of (○) MCM-41, (△) BM-200, (◇) BM-300, (●) BM-400 and (□) BM-500.

(Fig. 5b) shows the contribution of pyridine adducts in the region of 1400–1650 cm^{-1}. In this spectrum, the peaks at 1448 and 1598 cm^{-1} are attributed to pyridine bonded Lewis acid sites of the BM-400. These peaks are overlapped with the peaks of O–B at 1408 cm^{-1} and the peak of water at 1632 cm^{-1}, respectively. The weak peak at 1478 cm^{-1} is the combination band of pyridine bonded to Lewis and Brønsted acid sites. The characteristic peak of Brønsted acid site (1543 cm^{-1}) is not detected in the spectrum. This is due to the presence of much higher numbers of boron-containing Lewis acid sites relative to Brønsted acid sites. The peak at 1635 cm^{-1} in the spectrum of the catalyst before pyridine adsorption (Fig. 5a) and also after pyridine adsorption is due to the presence of water on the preparation of the pellet sample. This sharp peak may overlap with the weak peak of the Brønsted acid site at 1635 cm^{-1}. These results suggest that the Lewis acid sites have a dominant role in the catalytic activity.

In order to compare the strength of the acidic sites of BM samples, FT-IR spectra of pyridine-adsorbed BM samples before heat treatment and after heating at 200 °C are shown in Fig. 6. All samples before heat treatment show peaks of Lewis acid sites and a weaker peak of Brønsted acid sites (Fig. 6a–d). However, after heating at 200 °C, only BM-400 shows the strong peaks of Lewis acid sites (Fig. 6h) and the other spectra show desorption of pyridine at this temperature (Fig. 6e–g). These results confirm strong acid sites of BM-400 compared with other samples.

The loading amount of BF_3 on the BM-400 was determined by a spectrophotometric method[26] and results are shown in Table 1. To investigate the bonding state of BF_3 and B/F mole ratios on the MCM-41 before and after heat treatment, the fluoride contents of BM-120 and BM-400 were measured by a potentiometric method using a fluoride ion-selective electrode.[27] By this method, the B/F mole ratios for BM-120 and BM-400 were obtained as 1/1.98 ≈ 1/2 and 1/2.91 ≈ 1/3, respectively. These results confirm the presence of BF_3 on the surface of BM-120 with bonding interaction between the oxygen of silanol or Si–O–Si and the boron of BF_3. The B/F mole ratio of 1/2 in BM-400 also confirms the presence of a covalent bond between the oxygen of Si–O and boron and formation of –O–BF_2 due to evolution of HF during calcination. Thus, Si–O–BF_2 is the final structural form of the catalyst in BM-400. This results are confirmed by the shift of the B–O stretching vibration from 1392 cm^{-1} in BM-120 (Fig. 2b) to 1408 cm^{-1} in BM-400 (Fig. 2c), which is due to transformation of the weaker coordinated bond of O–B in BM-120 to a stronger covalent bond in BM-400.

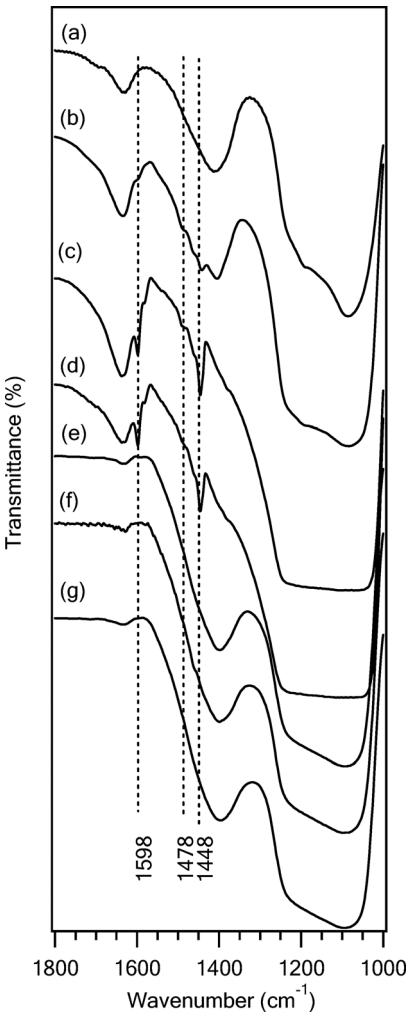

Fig. 5 FT-IR spectra of (a) BM-400 and pyridine-adsorbed BM-400 at: (b) 25 °C, (c) 100 °C, (d) 200 °C, (e) 300 °C, (f) 400 °C and (g) 500 °C.

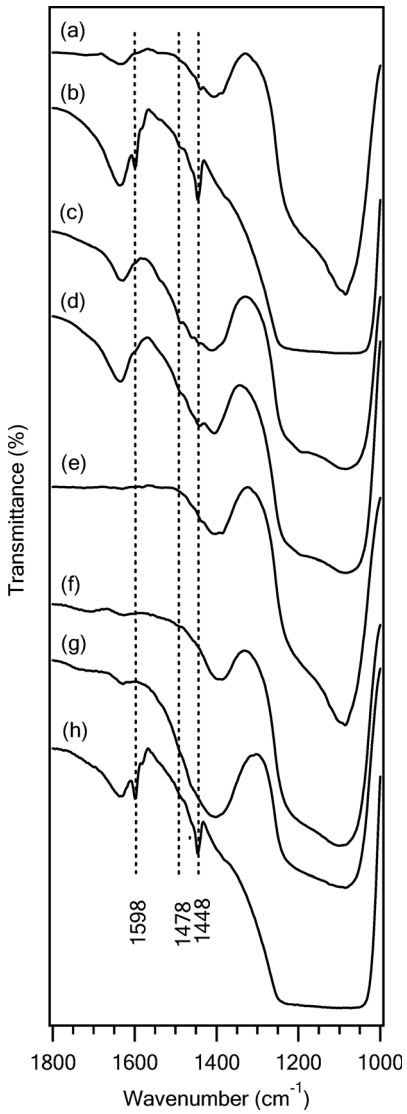

Fig. 6 FT-IR spectra of pyridine-adsorbed (a) BM-120, (b) BM-200, (c) BM-300 and (d) BM-400 at ambient temperature and (e) BM-120, (f) BM-200, (g) BM-300 and (h) BM-400 at 200 °C.

3.2. Catalytic activity of BF_3/MCM-41

The catalytic activity of BF_3/MCM-41 nanoparticles was investigated in the synthesis of 3-imidazo[1,2-a]pyridines. Initially, the reaction of benzaldehyde, trimethylsilyl cyanide and 2-aminopyridine was selected as the model reaction. The maximum loading amount of BF_3 on the MCM-41 (20 wt.%) was achieved by impregnation of MCM-41 using a suspension containing BF_3:MCM-41 mole ratio of 5 : 1 (Table 1). As shown in Table 1, a higher concentration of $BF_3{\cdot}Et_2O$ in the impregnation media cannot enhance the loading amount of BF_3 on the MCM-41. The effect of BF_3 loading amount in the catalytic activity of prepared samples was investigated in the model reaction. The results show that the catalytic activity in terms of reaction time and yields of the products were increased by an increase in the loading of BF_3 up to 20 wt.% (Table 1, entry 3).

Thus, further optimization experiments were performed using BF_3/MCM-41 prepared with 1 : 5 mole ratio (BM samples) and the results are shown in Table 2.

To investigate the effect of the calcination temperature on the catalytic activity, the model reaction was carried out in the presence of 100 mg of BM samples (Table 2, entries 1–5).

As shown in Table 2 (entry 5), with increase in calcination temperature up to 400 °C, the reaction times were decreased and the yields were increased. The reaction time was increased and the yield was decreased with further increase in calcination temperature (Table 2, entry 6). These results indicate that BM-400 has the best catalytic activity.

In order to optimize the amount of BM-400 on the catalytic performance, the model reaction was also carried out in the presence of various amounts of BM-400 and the results show that in terms of reaction time and the yield, the use of 50 mg of BM-400 has the best performance (Table 2, entry 8).

To investigate the effect of the solvent on the catalytic reaction, the model reaction in the presence of 50 mg of

Table 1 Catalytic activity of 100 mg BM-400 with various loading amounts of BF_3 in the synthesis of imidazo[1,2-a]pyridine

Entry	BF_3: MCM-41 (mole ratio)[a]	BF_3 loading[b] (Mole ratio)	(wt.%)	Time (min)	Yield (%)
1	1 : 15	0.053	6	70	75
2	1 : 10	0.11	13	60	85
3[c]	1 : 5	0.181	20	45	95
4	1 : 4	0.181	20	45	95
5	1 : 3	0.181	20	45	95
6[d]	—	0.181	20	60	90

[a] Mole ratio in the sample preparation media. [b] Loading of BF_3 on the MCM-41 was determined by spectrophotometric method.[26] [c] Selected catalyst. [d] Reused catalyst.

BM-400 was carried out in various solvents under reflux conditions (Table 2, entries 8, 10–13). The result show that the EtOH is the best solvent in terms of the time and yield (Table 2, entry 8). The model reaction was also performed under solvent-free conditions and also at r.t. in EtOH. Results show low efficiency of these reactions (Table 2, entries 14–15). The efficiency of the BF_3 on the support was investigated by performing the reaction in the presence of pure MCM-41 and a low yield of the product was obtained (Table 2, entry 16). To show the effect of the support on the catalytic activity of BF_3, the model reaction was carried out in the presence of 11 mg $BF_3{\cdot}Et_2O$ as homogeneous analog and results show that a lower yield of product was achieved after a long time (Table 2, entry 17). The efficiency of the catalyst was also examined in a blank reaction, without any catalyst. The reaction was completed after 300 min with 50% yield of the product.

According to the optimization results, the reaction of benzaldehyde (2 mmol), TMSCN (1 mmol) and 2-aminopyridine (1 mmol) in the presence of 50 mg of BM-400 in EtOH under reflux conditions is best for the synthesis of imidazopyridines (Table 2, entry 8). The BM-400 catalyst under these conditions showed a turnover number (TON) of 7.14 moles of product per moles of catalyst.

The scope and generality of this type of reaction is illustrated with respect to the reaction of different aldehydes and 2-aminopyridines with TMSCN and the results are summarized in the Table 3.

As shown in Table 3, various type of aldehydes with both electron-donating and electron-withdrawing substituents were reacted with TMSCN and 2-aminopyridine under the same reaction conditions and the corresponding imidazopyridines were obtained in high yields (Table 3, entries **4a–i**). The work-up and recovery of the catalyst are simple. After completion of the reaction (monitored by TLC; eluent: EtOAc : *n*-hexane, 25 : 75), the catalyst was separated by centrifuge and was washed by EtOH (3 × 5 mL). The crude product was recrystallized by EtOH to obtain pure imidazo[1,2-a]pyridine.

Reusability is one of the most important features of a solid acid catalyst. To investigate this trait, the recovered catalyst from the model reaction was dried in an oven at 120 °C for 2 h. The recovered catalyst was reused in the model reaction. The obtained result shows a moderate increase in the reaction time and yield of the product (Table 4, entry 2).

This moderate deactivation may be due to partial blockage of the active sites of the catalyst or leaching of boron from the surface. To clarify the reason for the decline in activity, the BF_3 loading of the recovered catalyst was determined and the results show 20 wt% BF_3 on the MCM-41 (Table 1, entry 6). This result confirms that leaching is not the reason for deactivation. However, the recovered catalyst in run 4 was calcined at 400 °C for 2 h and then reused in the same reaction. The result shows that the catalytic activity was increased almost to that of the fresh catalyst. This confirms that deactivation is due to blockage of the active sites of the catalyst. It should be noted that at 400 °C the calcination may be incomplete and partial blockage may remain.

Table 2 Optimization of the reaction conditions for the synthesis of imidazo[1,2-a]pyridine in the presence of BF_3/MCM-41

Entry	Catalsyst	Solvent	Catalyst amount (mg)	Time (min)	Yield (%)
1	BM-120	EtOH	100	40	95
2[a]	BM-120	EtOH	100	100	85
3	BM-200	EtOH	100	135	80
4	BM-300	EtOH	100	120	85
5	BM-400	EtOH	100	45	95
6	BM-500	EtOH	100	55	85
7	BM-400	EtOH	25	120	95
8	BM-400	EtOH	50	50	95
9	BM-400	EtOH	75	50	95
10	BM-400	MeOH	50	50	95
11	BM-400	CH_3CN	50	240	40
12	BM-400	$CHCl_3$	50	90	55
13	BM-400	CH_2Cl_2	50	90	58
14[b]	BM-400	—	50	60	85
15[c]	BM-400	EtOH	50	240	85
16	MCM-41	EtOH	50	240	50
17	$BF_3{\cdot}Et_2O$	EtOH	21	180	74

[a] Results of reused BM-120. [b] The reaction was performed at 80 °C. [c] The reaction was performed at room temperature.

Table 3 Reaction of aldehydes, 2-aminopyridines and TMSCN for the synthesis of 3-imidazo[1,2-a]pyridines in the presence of BM-400

Entry	Aldehyde (1)	2-Aminopyridine (2)	Imidazo[1,2-a]pyridine (4)	Time (min)	Yield (%)	Mp (°C) Ref.
4a	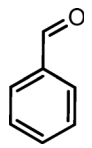	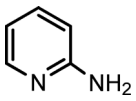	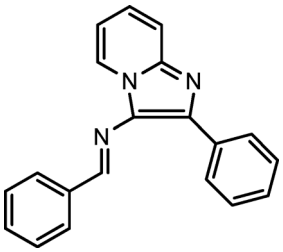	50	95	160–163[28]
4b	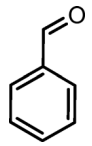	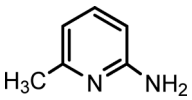	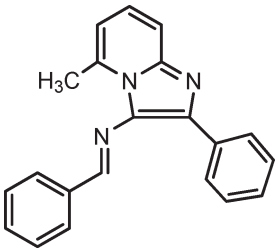	180	75	135–138[13]
4c	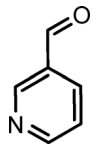	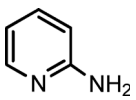	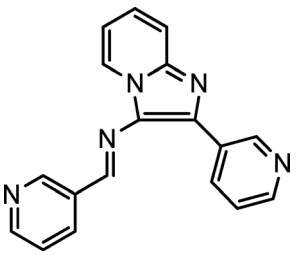	50	85	200–204[11]
4d	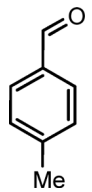	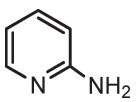	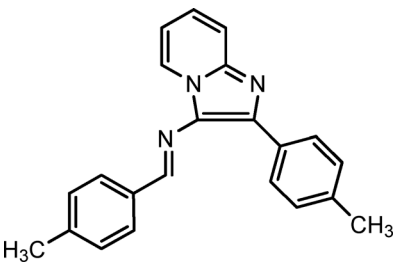	90	80	155–157[28]
4e	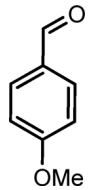	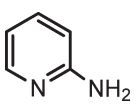	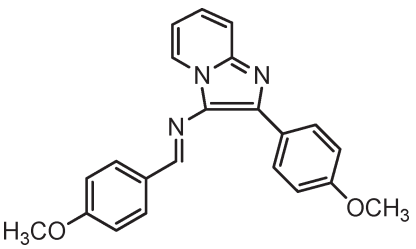	75	80	172–176[28]
4f	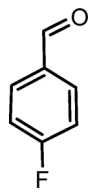	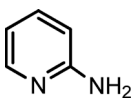	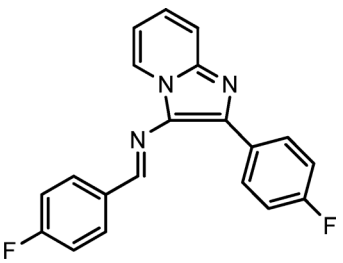	90	80	158–160[29]

Table 3 *(continued)*

Entry	Aldehyde (1)	2-Aminopyridine (2)	Imidazo[1,2-a]pyridine (4)	Time (min)	Yield (%)	Mp (°C) Ref.
4g	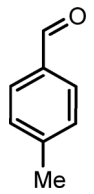	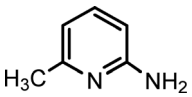	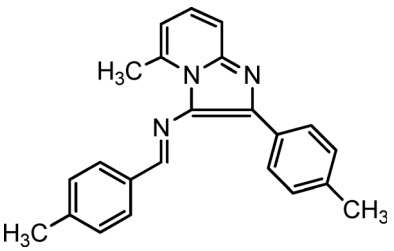	70	85	135–138[28]
4h	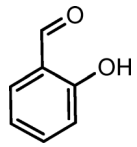	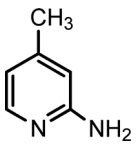	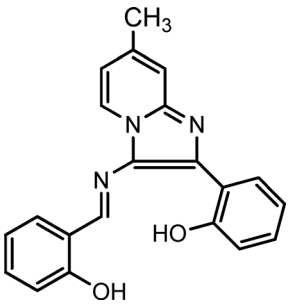	50	80	211–213[13]
4i	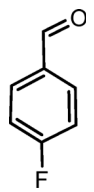	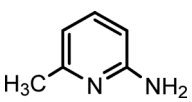	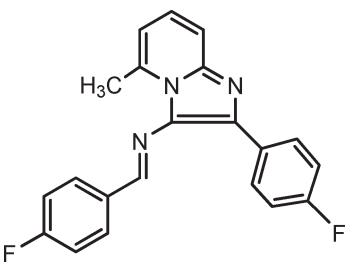	90	75	150–152[28]

Table 4 Reusability of BM-400 in reaction of 2-aminopyridine, benzaldehyde and TMSCN for the synthesis of [1,2-a]pyridines

Entry	Catalyst amount (mg)	Time (min)	Yield[a] (%)
1	50	50	95
2	50	60	90
3	50	70	87
4	50	75	80
5[b]	50	55	90

[a] Isolated yield. [b] The catalyst was calcined before use at 400 °C for 2 h.

4. Conclusion

In conclusion, we have demonstrated that BF_3 on the surface of MCM-41 can be used as an efficient solid acid catalyst for the synthesis of imidazopyridines. High yields of the products, simple work-up, reusability and simple purification of the products are advantages of this procedure.

Acknowledgements

We are thankful to the Yazd University Research Council for partial support of this work.

References

1 Y. Maruyama, K. Anami, M. Terasawa, K. Goto, T. Imayoshi, Y. Kadobe and Y. Mizushima, *Arzneim. Forsch.*, 1981, **31**, 1111–1118.
2 R. B. Lacerda, C. K. de Lima, L. L. da Silva, N. C. Romeiro, A. L. Miranda, E. J. Barreiro and C. A. Fraga, *Bioorg. Med. Chem.*, 2009, **17**, 74–84.
3 A. Özdemir, G. Turan-Zitouni, Z. Asım Kaplancıklı, G. İşcan, S. Khan and F. Demirci, *Eur. J. Med. Chem.*, 2010, **45**, 2080–2084.
4 J.-M. Chezal, J. Paeshuyse, V. Gaumet, D. Canitrot, A. Maisonial, C. Lartigue, A. Gueiffier, E. Moreau, J.-C. Teulade, O. Chavignon and J. Neyts, *Eur. J. Med. Chem.*, 2010, **45**, 2044–2047.
5 S. Ulloora, R. Shabaraya, S. Aamir and A. V. Adhikari, *Bioorg. Med. Chem. Lett.*, 2013, **23**, 1502–1506.
6 R. Menegatti, G. M. S. Silva, G. Zapata-Sudo, J. M. Raimundo, R. T. Sudo, E. J. Barreiro and C. A. M. Fraga, *Bioorg. Med. Chem.*, 2006, **14**, 632–640.
7 C. Blackburn, *Tetrahedron Lett.*, 1998, **39**, 5469–5472.
8 H. Bienaymé and K. Bouzid, *Angew. Chem., Int. Ed.*, 1998, **37**, 2234–2237.
9 K. Groebke, L. Weber and E. Mehlin, *Synlett*, 1998, **661**, 3635–3638.

10 J. Schwerkoske, T. Masquelin, T. Perun and C. Hulme, *Tetrahedron Lett.*, 2005, **46**, 8355–8357.
11 T. Masquelin, H. Bui, B. Brickley, G. Stephenson, J. Schwerkoske and C. Hulme, *Tetrahedron Lett.*, 2006, **47**, 2989–2991.
12 A. Shaabani and A. Maleki, *Monatsh. Chem.*, 2007, **138**, 51–56.
13 A. I. Polyakov, V. A. Eryomina, L. A. Medvedeva, N. I. Tihonova, A. V. Listratova and L. G. Voskressensky, *Tetrahedron Lett.*, 2009, **50**, 4389–4393.
14 J. S. Beck, J. C. Vartuli, W. J. Roth, M. E. Leonowicz, C. T. Kresge, K. D. Schmitt, C. T. W. Chu, D. H. Olson and E. W. Sheppard, *J. Am. Chem. Soc.*, 1992, **114**, 10834–10843.
15 K. G. Bhattacharyya, A. K. Talukdar, P. Das and S. Sivasanker, *Catal. Commun.*, 2001, **2**, 105–111.
16 M. Abdollahi-Alibeik and M. Pouriayevali, *React. Kinet., Mech. Catal.*, 2011, **104**, 235–248.
17 J. Zhou, R. Zhou, L. Mo, S. Zhao and X. Zheng, *J. Mol. Catal. A: Chem.*, 2002, **178**, 289–292.
18 A. Procopio, G. Das, M. Nardi, M. Oliverio and L. Pasqua, *ChemSusChem*, 2008, **1**, 916–919.
19 X. Dong, L. Wang, G. Jiang, Z. Zhao, T. Sun, H. Yu and W. Wang, *J. Mol. Catal. A: Chem.*, 2005, **240**, 239–244.
20 M. M. Heravi, B. Baghernejad, H. A. Oskooie and R. Malakooti, *J. Chin. Chem. Soc.*, 2008, **55**, 1129–1132.
21 M. Abdollahi-Alibeik and M. Pouriayevali, *Catal. Commun.*, 2012, **22**, 13–18.
22 M. Abdollahi-Alibeik and F. Nezampour, *React. Kinet., Mech. Catal.*, 2013, **108**, 213–229.
23 K. Wilson and J. H. Clark, *Chem. Commun.*, 1998, 2135–2136.
24 M. Abdollahi-Alibeik and E. Heidari-Torkabad, *C. R. Chim.*, 2012, **15**, 517–523.
25 I. Mohammadpoor-Baltork, V. Mirkhani, M. Moghadam, S. Tangestaninejad, M. A. Zolfigol, M. Abdollahi-Alibeik, A. R. Khosropour, H. Kargar and S. F. Hojati, *Catal. Commun.*, 2008, **9**, 894–901.
26 W. Dible, E. Truog and K. Berger, *Anal. Chem.*, 1954, **26**, 418–421.
27 W. Frenzel and P. Brätter, *Anal. Chim. Acta*, 1986, **188**, 151–164.
28 M. Adib, E. Sheibani, H. R. Bijanzadeh and L.-G. Zhu, *Tetrahedron*, 2008, **64**, 10681–10686.
29 M. Adib, E. Sheibani, L.-G. Zhu and P. Mirzaei, *Tetrahedron Lett.*, 2008, **49**, 5108–5110.